J Mol Model (2006) 12: 621–629
DOI 10.1007/s00894-005-0029-3

ORIGINAL PAPER

Alexander Alex · Elke Hänsele · Timothy Clark

# The ethylene/metal(0) and ethylene/metal(I) redox system: model ab initio calculations

Received: 19 December 2004 / Accepted: 8 July 2005 / Published online: 9 December 2005


**Abstract** Ab initio calculations (coupled cluster with single and double excitations; CCSD) have been used to investigate the model redox systems ethylene:M(0) (M = Li, Na, K, Rb, Cs) and ethylene:M(I) (M = Be, Mg, Ca, Sr, Ba, Zn, Cd, Hg). Within $C_{2v}$ symmetry, the ground ($^2A_1$) states correspond to the charge distribution given in the title. The lowest ($^2B_2$) excited states correspond, somewhat counter intuitively, to the ethylene$^{\bullet-}$/M(II) ion pair.These trends can be rationalized on the basis of simple electrostatic and configuration-mixing arguments that lead to two simple equations for predicting the electron-transfer energies for oxidation or reduction of the ethylene. The electron-transfer energies to the $^2B_2$ ion pairs are dominated by the electrostatic ion-pairing energies.

**Keywords** Electron transfer · Ab initio · CCSD(T) · Ethylene

## Introduction

We have shown previously [1–3] that the catalysis of simple closed-shell reactions by Group II metal radical cations can be explained as the result of electron transfer from the metal to the substrate during the reactions. This electron transfer is also known experimentally for transition-metal complexes [4–7] and the resulting geometrical changes in the substrates have been studied extensively [8]. In this paper we focus our attention on electron transfer from different Group II and Group XII metal radical cations to ethylene as a model system in order to understand this type of catalysis better. We will show that the energy required for electron transfer is governed mainly by simple electrostatic interactions and physical properties of the metals such as ionization potentials and ionic radii.

We now report model ab initio molecular orbital calculations on electron-transfer reactions of the ground state ($^2A_1$ in $C_{2v}$ symmetry) complexes $M^{\bullet}:C_2H_4$ (M = Li, Na, K, Rb, Cs) and $M^{\bullet+}:C_2H_4$ (M = Be, Mg, Ca, Sr, Ba, Zn, Cd, Hg). Electron transfer from the metal to ethylene (the reductive process) leads to the first excited ($^2B_2$ in $C_{2v}$ symmetry) $M^{+}:C_2H_4^{\bullet-}$ and $M^{2+}:C_2H_4^{\bullet-}$ states. Transfer of an electron from the ethylene to the metal (the oxidative process) leads to a higher-lying $^2A_1$ excited state, as shown in Scheme 1, where the three relevant molecular orbitals (MOs) and their occupancies in the three different states are shown schematically. For the purposes of this analysis, and for most of our calculations, we have constrained the structures to $C_{2v}$ symmetry. In most cases, the $C_{2v}$ structures are also minima, as shown below.

The bonding combination ($\Psi_1$) of the ethylene $\pi$-HOMO and the *s*-orbital of the metal is concentrated on the olefin, as shown in Scheme 1, as long as the ionization potential of the metal is significantly lower than that of ethylene (10.51 eV, 242.4 kcal mol$^{-1}$) [9]. The corresponding antibonding combination, $\Psi_2$, is thus concentrated on the metal so that the excitation of an electron from $\Psi_1$ to $\Psi_2$ essentially corresponds to electron transfer from the olefin to the metal, which we have called the oxidative process. This redox process is intuitively attractive in the gas phase because it involves only a charge shift, not a separation of charges. The ethylene $\pi^*$-LUMO can possibly interact weakly with a metal *P*- (or even *d*-) orbital, as shown in $\Psi_3$ of Scheme 1. Excitation of an electron from $\Psi_2$

Dedicated to Paul Schleyer on the occasion of his 75th Birthday

A. Alex
Medicinal Informatics, Structure and Design,
Pfizer Global Research and Development,
Sandwich Laboratories, Ramsgate Road,
Sandwich CT13 9NJ, UK

E. Hänsele · T. Clark (✉)
Computer-Chemie-Centrum der Universitaet
Erlangen-Nuernberg, Naegelsbachstrasse 25,
91052 Erlangen, Germany
E-mail: clark@chemie.uni-erlangen.de
Tel.: +49-9131-8522948
Fax: +49-9131-8526565

**Scheme 1** Schematic view of the orbital occupations for the three states discussed in the text

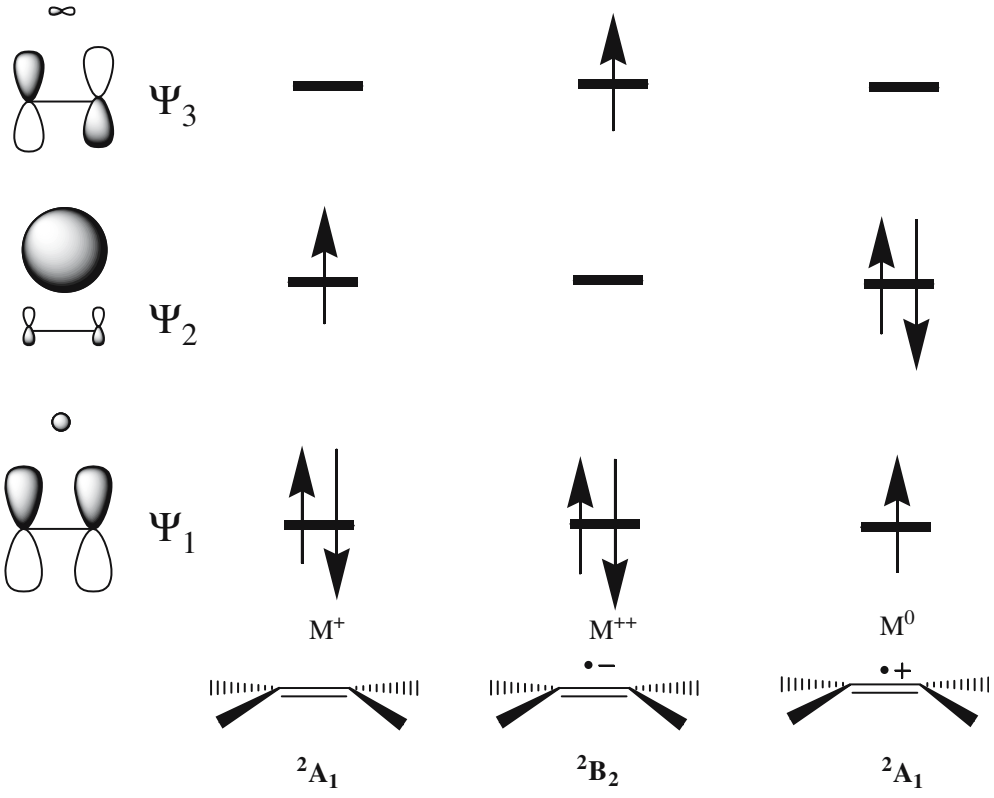


(metal centered) to $\Psi_3$ (ethylene $\pi^*$), therefore, represents an electron transfer from the metal to the olefin, which we have denoted the reductive process. At first sight this redox option is less attractive than the oxidative process because it involves charge separation. However, the product is an intimate ion pair so that Coulomb attraction between the ions can play a significant role. We now report calculations designed to assess the roles of the different physical parameters in determining the redox behavior of ethylene:metal systems.

There have been several theoretical studies of ground-state metal:ethylene complexes. As far as we are aware, Trenary et al. [10] were the first to study Li:ethylene in detail. They investigated both the $^2A_1$ and the $^2B_2$ states and found the latter to be the ground state and to be bound by 18 kcal mol$^{-1}$. We [11] later investigated reductive electron transfer from alkali metal atoms to ethylene and were able to describe the energy required for this process in terms of a simple electrostatic model. Using a diffuse-augmented basis set, we found $^2A_1$ to be the ground state with $^2B_2$ as the first excited state 9.7 kcal mol$^{-1}$ (CISD/6-31++G*//UHF/6-31++G*) higher in energy. A later DFT/coupled cluster study [12] of $C_{2v}$ Li:ethylene concluded that the ground state was $^2B_2$, in contrast to our previous findings. We suspect that the reason for these discrepancies is basis set superposition error (BSSE) in Refs. [10, 12], which did not use diffuse-augmented basis sets for ethylene. In both cases, the authors were not able to optimize the geometries correctly so that this may also be a source of the disagreement. Our results reported below confirm those of our earlier work that the ground state of $C_{2v}$ Li:ethylene is $^2A_1$. However, experimental work in an argon matrix [13, 14] reveals a $^2B_2$ ground state. We have, however, pointed out [11] that solvation, even by a nonpolar but polarizable solvent such as argon, favors the $^2B_2$ state over the nonpolar $^2A_1$. We will return to the question of the ground state of $C_{2v}$ Li:ethylene below.

Calculations on Na:ethylene and K:ethylene were also reported in Refs. [11, 12]. In both cases, the $^2A_1$ state was found to be more stable. However, a CASSCF study of Na:ethylene [15] later reported results consistent with a $^2B_2$ state. Once again, this study did not use a diffuse-augmented basis set so that it may artificially favor the $^2B_2$ configuration because of BSSE. We have not been able to find previous calculations on Rb:ethylene and Cs:ethylene. Note that calculations on the $\beta$-lithium [16, 17] and sodium [17] substituted ethyl radicals have also been reported.

Calculational studies on the complexes of ethylene with Group II and Group XII radical cations are less common. Balaji and Jordan [18] investigated the insertion of Be and Mg atoms with acetylene and ethylene and included $C_2H_4Be^{\bullet+}$ and $C_2H_4Mg^{\bullet+}$ in their study. As far as we are concerned, electron transfer in $Be^{\bullet+}$:ethylene and $Mg^{\bullet+}$:ethylene has not been investigated. Calculations involving ethylene and the coinage metals have concentrated on the neutral metal atoms.

**Table 1** Calculated total energies and ionization potentials (IP) for the metal atoms and ions used in this work

| Species | Exp. IP [43] (kcal mol$^{-1}$) | CCSD | | CCSD(T) | |
|---|---|---|---|---|---|
| | | Total energy (a.u.) | IP (kcal mol$^{-1}$) | Total energy (a.u.) | IP (kcal mol$^{-1}$) |
| Li | 123.0 | −7.43203 | 123.1 | −7.43203 | 123.1 |
| $Li^+$ | | −7.23584 | | −7.23584 | |
| Na | 114.0 | −161.84598 | 114.0 | −161.84598 | 114.0 |
| $Na^+$ | | −161.66429 | | −161.66429 | |
| K | 100.0 | −599.33270 | 97.7 | −599.33604 | 98.0 |
| $K^+$ | | −599.17697 | | −599.17983 | |
| Rb | 96.3 | −23.82486 | 88.8 | −23.82503 | 88.8 |
| $Rb^+$ | | −23.68336 | | −23.68349 | |
| Cs | 89.8 | −19.86914 | 81.7 | −19.86927 | 81.7 |
| $Cs^+$ | | −19.73900 | | −19.73911 | |
| $Be^{\bullet+}$ | 420.0 | −14.27620 | 417.8 | −14.27620 | 417.8 |
| $Be^{2+}$ | | −13.61038 | | −13.61038 | |
| $Mg^{\bullet+}$ | 346.7 | −199.36389 | 338.8 | −199.36389 | 338.8 |
| $Mg^{2+}$ | | −198.82299 | | −198.82299 | |
| $Ca^{\bullet+}$ | 273.3 | −36.49760 | 271.5 | −36.50167 | 272.0 |
| $Ca^{2+}$ | | −36.06490 | | −36.06824 | |
| $Sr^{\bullet+}$ | 254.4 | −30.30922 | 250.6 | −30.31060 | 250.9 |
| $Sr^{2+}$ | | −29.90980 | | −29.91081 | |
| $Ba^{\bullet+}$ | 230.7 | −25.06024 | 222.5 | −25.06372 | 222.8 |
| $Ba^{2+}$ | | −24.70572 | | −24.70860 | |
| $Zn^{\bullet+}$ | 414.3 | −1777.73606 | 399.6 | −1777.74408 | 400.7 |
| $Zn^{2+}$ | | −1777.09917 | | −1777.10547 | |
| $Cd^{\bullet+}$ | 389.8 | −166.66930 | 370.3 | −166.67226 | 370.8 |
| $Cd^{2+}$ | | −166.07922 | | −166.08137 | |
| $Hg^{\bullet+}$ | 432.5 | −152.33820 | 409.5 | −152.34073 | 410.0 |
| $Hg^{2+}$ | | −151.68566 | | 151.68735 | |

## Calculations

Geometry optimizations were the first performed within $C_{2v}$ symmetry with Gaussian03 [19] at the coupled cluster with single and double excitations (CCSD) level [20–23]. Where available (H, C, Li, Na, K, Be, Mg and Zn), the 6-311 + G(d,p) basis set [24–31] was used. For the other metals, the Stuttgart/Dresden SDD basis sets and pseudopotentials [32–33] were used. The optimized structures were characterized as minima, saddle points or higher stationary points by calculating their normal vibrations within the harmonic approximation by numerical differentiation of the analytical CCSD first derivatives. If the $C_{2v}$ structure was not found to be a minimum, minima of lower symmetry were sought. The energies were refined by CCSD(T) calculations [34] at the CCSD-optimized geometries.

## Results

Table 1 shows the results obtained for calculations of the relevant ionization potentials for this work.

The trends are consistent throughout the table. Both first and second ionization potentials are reproduced well for the lighter elements and errors increase (ionization potentials are underestimated) for the heavier metals. The error increases steadily up to one electron

**Table 2** CCSD/6-311 + G(d,p) optimized carbon–carbon bond lengths (C = C, Å), carbon–metal distances (C...M, Å), C = C–H angles ( ∠CCH, °) and metal–C–C–H dihedral angles (∅M...CCH, °) for the $^2A_1$ metal:ethylene complexes

| | Li | Na | K | Rb | Cs |
|---|---|---|---|---|---|
| C = C | 1.340 | 1.340 | 1.340 | 1.351 | 1.339 |
| C...M | 4.651 | 4.900 | 4.598 | 3.466 | 4.615 |
| ∠CCH | 121.6 | 121.6 | 121.6 | 121.7 | 121.6 |
| ∅M...CCH | 90.1 | 90.1 | 90.3 | 90.7 | 90.5 |
| | $Be^{\bullet+}Be^{+\cdot}$ | $Mg^{\bullet+}$ | $Ca^{\bullet+}$ | $Sr^{\bullet+}$ | $Ba^{\bullet+}$ |
| C = C | 1.365 | 1.353 | 1.347 | 1.346 | 1.345 |
| C...M | 1.956 | 2.677 | 3.057 | 3.315 | 3.442 |
| ∠CCH | 121.4 | 121.4 | 121.4 | 121.4 | 121.4 |
| ∅M...CCH | 95.8 | 95.6 | 95.6 | 95.3 | 95.2 |
| | $Zn^{\bullet+}$ | $Hg^{\bullet+}$ | $Cd^{\bullet+}$ | | |
| C = C | 1.361 | 1.368 | 1.358 | | |
| C...M | 2.492 | 2.651 | 2.702 | | |
| ∠CCH | 121.2 | 121.0 | 121.1 | | |
| ∅M...CCH | 95.7 | 96.6 | 96.1 | | |

**Table 3** Total energies (a.u), number of imaginary normal vibrations (NIMAG), lowest frequency ($\nu_1$, $cm^{-1}$), zero-point vibrational energies (ZPE, kcal $mol^{-1}$) and complexation energies (metal + ethylene → complex, corrected using the unscaled CCSD-ZPE, kcal $mol^{-1}$) for the $^2A_1$ metal:ethylene complexes

| Metal | CCSD | | | | | CCSD(T) | |
|---|---|---|---|---|---|---|---|
| | Total energy | NIMAG | $\nu_1$ | ZPE | $E_{comp.}$ | Total energy | $E_{comp.}$ |
| Li | −85.80643 | 0 | 19.8 | 32.07 | −0.11 | −85.81829 | −0.16 |
| Na | −240.22036 | 0 | 11.4 | 32.03 | −0.13 | −240.23220 | −0.17 |
| K | −677.70719 | 0 | 14.3 | 32.11 | −0.12 | −677.72244 | −0.21 |
| Rb | −102.20162 | 0 | 8.9 | 33.04 | −0.62 | −102.21401 | −0.26 |
| Cs | −98.24606 | 0 | 18.3 | 32.51 | −1.24 | −98.25845 | −0.55 |
| $Be^{\bullet+}$ | −92.71711 | 0 | 107.7 | 32.35 | −40.56 | −92.71940 | −35.61 |
| $Mg^{\bullet+}$ | −277.76548 | 0 | 81.7 | 32.90 | −16.33 | −277.77766 | −16.59 |
| $Ca^{\bullet+}$ | −114.89169 | 0 | 102.2 | 32.73 | −11.80 | −114.90847 | −12.38 |
| $Sr^{\bullet+}$ | −108.70019 | 0 | 90.3 | 32.62 | −9.95 | −108.71415 | −10.46 |
| $Ba^{\bullet+}$ | −103.45049 | 0 | 69.8 | 32.50 | −9.62 | −103.46653 | −10.11 |
| $Zn^{\bullet+}$ | −1856.14807 | 0 | 78.5 | 33.06 | −22.70 | −1856.16942 | −23.70 |
| $Cd^{\bullet+}$ | −245.07860 | 0 | 118.5 | 33.07 | −22.00 | −245.09489 | −21.98 |
| $Hg^{\bullet+}$ | −230.75905 | 0 | 112.7 | 33.19 | −29.13 | −230.77539 | −29.41 |

Volt for the second ionization potentials of mercury and is independent of whether the metal is treated in an all-electron calculation or using pseudopotentials. It is known [35, 36] that correlation is important for reproducing the second ionization potentials of metals and that a basis set adequate to allow an accurate description of core–valence correlation is important [37]. Errors found can be expected, both for the 6-311 + G(d,p) all-electron calculations with inflexible nonvalence basis functions and for the pseudopotential calculations.

## $^2A_1$ structures and complexation energies

Table 2 shows some geometrical details of the $^2A_1$ $C_{2v}$ complexes. The neutral complexes (those with alkali-metal atoms) all show the typical geometrical parameters of weak complexes, long C...M distances and an essentially unperturbed geometry for the ethylene moiety. The exception is the rubidium complex, which shows a larger deformation of the $C_2H_4$ unit. As expected from the theory of odd-electron bonds [38], the interaction between the metal and the olefin, and therefore also the perturbation of the olefin geometry, is far stronger for the singly charged (Group II and Group XII) complexes. The strengths of the interactions are shown in Table 3, which also give the total, zero-point and complexation energies.

As expected [38], the neutral complexes are all very weakly bound with complexation energies below 1 kcal $mol^{-1}$. The complexation energies of the cationic complexes should fall off exponentially with increasing difference between the first ionization potential of the metal and that of ethylene (ΔIP). Figure 1 shows a plot of ΔIP vs. $\log_{10}(E_{comp})$. There is a good linear correlation for all metals except beryllium, which can be expected to give a more negative complexation energy because it is the only first-row element [38]. Thus, the complexation energies between the metals and ethylene in the $^2A_1$ state behave exactly as expected for three-

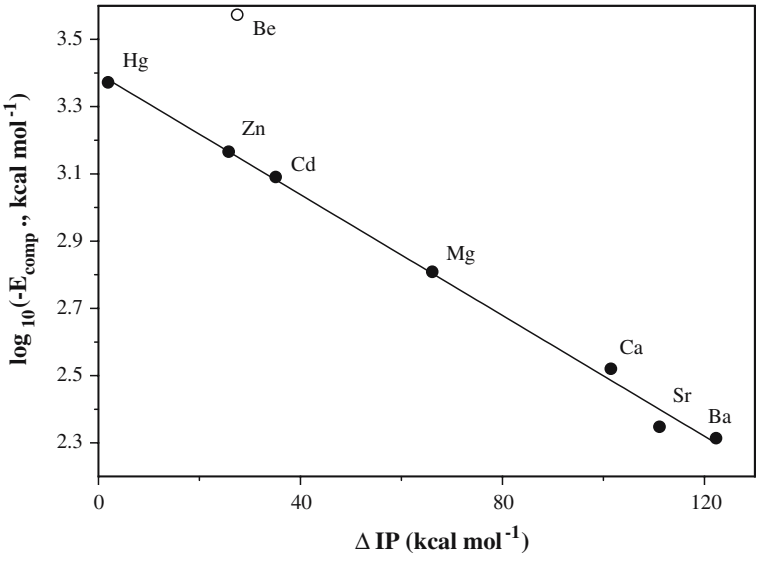


**Fig. 1** Plot of the logarithm of the calculated complexation energies (CCSD(T), Table 3) against the differences in first ionization potential between the metal and ethylene (experimental values)

**Table 4** CCSD/6-311 + G(d,p) optimized carbon–carbon bond lengths (C = C, Å), carbon–metal distances (C...M, Å), C = C–H angles ( ∠CCH, °) and metal–C–C–H dihedral angles (∅M...CCH, °) for the $^2B_2$ metal:ethylene complexes

| | Li | Na | K | Rb | Cs |
|---|---|---|---|---|---|
| C = C | 1.435 | 1.444 | 1.437 | 1.351 | 1.346 |
| C...M | 2.070 | 2.441 | 2.788 | 3.466 | 3.761 |
| ∠CCH | 119.6 | 119.2 | 119.2 | 121.7 | 121.7 |
| ∅M...CCH | 104.1 | 105.6 | 105.8 | 91.9 | 91.5 |
| | $Be^{\bullet+}$ | $Mg^{\bullet+}$ | $Ca^{\bullet+}$ | $Sr^{\bullet+}$ | $Ba^{\bullet+}$ |
| C = C | 1.464 | 1.480 | 1.438 | 1.433 | 1.406 |
| C...M | 1.756 | 2.163 | 2.423 | 2.591 | 2.768 |
| ∠CCH | 119.3 | 118.6 | 119.1 | 119.2 | 120.1 |
| ∅M...CCH | 102.4 | 106.0 | 105.5 | 105.4 | 105.4 |
| | $Zn^{\bullet+}Zn^{+\cdot}$ | $Hg^{\bullet+}$ | $Cd^{\bullet+}$ | | |
| C = C | 1.502 | 1.531 | 1.501 | | |
| C...M | 2.057 | 2.271 | 2.263 | | |
| ∠CCH | 118.6 | 118.3 | 118.5 | | |
| ∅M...CCH | 104.5 | 104.7 | 105.1 | | |

electron interactions. Note that the different behaviors of Groups II and XII with respect to the dependence of $\Delta E_{comp}$ on atomic number parallels the behavior of the relevant ionization potentials.

The good correlation shown in Fig. 1 suggests that the individual $\lambda$-values [35] of the original equation are very similar for the seven metals included in the correlation, which in turn suggests that they all have very similar symmetrical three-electron bond energies [39], which seems very reasonable.

## $^2B_2$ structures and electron-transfer energies

Table 2 shows some geometrical details of the $^2A_1$ $C_{2v}$ complexes.

With the exception of Rb and Cs, the complexes all have the expected structures for $M^{2+}$:ethylene$^{\bullet-}$ ion pairs. An ion pair of this type can be optimized at the UHF/6-311 + G(d,p) level for M = Rb and Cs, but at the CCSD level, this collapses to the structure described in Table 4, which is a nonpolar $^2B_2$ complex between neutral ethylene and a $^2P$ metal atom.

All other Group I and II structures correspond to the ion-pair configuration with long (1.43–1.48 Å) C–C bonds, short C–metal distances and significantly nonplanar $C_2H_4$ moieties. The Group XII metals give significantly longer (1.50–1.53 Å) C–C bonds, suggesting that these complexes can be seen as metallacyclopropanes.

All $C_{2v}$ structures except that for M = $Mg^{\bullet+}$ are found to be minima. We were unable to find a minimum of any symmetry corresponding to an $M^{2+}$:ethylene$^{\bullet-}$ ion pair and have therefore used the energy for the $C_{2v}$ transition state in the remainder of the discussion. Note that this does not mean that we were unable to find a minimum but rather that distorting $C_2H_4Mg^+$ from the $C_{2v}$ structure is accompanied by a change in the electronic character to that corresponding to a distorted $^2A_1$ state. The electron-transfer energies range from 2–3 (for Li and $Be^{\bullet+}$) to 53 $\left(Hg^{\bullet+}\right)$ kcal mol$^{-1}$. Perhaps most remarkably, $Be^{\bullet+}$ is found to be able to reduce ethylene as well as Li. In these two cases, we find the $^2A_1$ state to be slightly lower in energy than the $^2B_2$, but the assignment must be considered tentative because of the small calculated energy differences.

**Table 5** Total energies (a.u), number of imaginary normal vibrations (NIMAG), lowest frequency ($\nu_1$, cm$^{-1}$), zero-point vibrational energies (ZPE, kcal mol$^{-1}$) for the $^2B_2$ metal:ethylene complexes and electron-transfer ($^2A_1 \rightarrow {}^2B_2$complex, corrected using the unscaled CCSD–ZPE, kcal mol$^{-1}$)

| Metal | CCSD | | | | | CCSD(T) | |
|---|---|---|---|---|---|---|---|
| | Total energy | NIMAG | $\nu_1$ | ZPE | $\Delta E_{ET}$ | Total energy | $\Delta E_{ET}$ |
| Li | −85.80128 | 0 | 390.7 | 31.86 | 3.02 | −85.81342 | 2.85 |
| Na | −240.18512 | 0 | 156.5 | 30.68 | 20.76 | −240.19748 | 20.44 |
| K | −667.66442 | 0 | 254.3 | 30.64 | 24.92 | −677.68492 | 22.06 |
| Rb | −102.15853 | 0 | 93.7 | 32.17 | 26.17 | −102.17117 | 26.01 |
| Cs | −98.20663 | 0 | 77.1 | 32.32 | 24.56 | −98.21916 | 24.46 |
| $Be^{\bullet+}$ | −92.70336 | 0 | 489.5 | 32.30 | 8.58 | −92.71584 | 2.18 |
| $Mg^{\bullet+}$ | −277.71385 | 1 | 251.6i | 31.67 | 32.40 | −277.72617 | 32.31 |
| $Cd^{\bullet+}$ | −114.86120 | 0 | 322.1 | 31.99 | 18.39 | −114.87907 | 17.71 |
| $Sr^{\bullet+}$ | −108.66642 | 0 | 288.3 | 31.73 | 20.31 | −108.68125 | 19.87 |
| $Ba^{\bullet+}$ | −103.44042 | 0 | 228.9 | 31.76 | 5.58 | −1856.08811 | 4.91 |
| $Zn^{\bullet+}$ | −1856.08811 | 0 | 440.2 | 33.07 | 37.63 | −1856.11062 | 36.91 |
| $Cd^{\bullet+}$ | −245.00481 | 0 | 380.6 | 32.53 | 45.76 | −245.02186 | 45.29 |
| $Hg^{\bullet+}$ | −230.67299 | 0 | 346.9 | 32.72 | 53.53 | −230.69040 | 52.86 |

**Table 6** Mulliken and natural population analysis (NPA [44]) charges calculated for the $^2B_2$ complexes

| M | Atomic charges | | Spin | M | Atomic charges | | Spin | M | Atomic charges | | Spin |
|---|---|---|---|---|---|---|---|---|---|---|---|
| | Mulliken | NPA | | | Mulliken | NPA | | | Mulliken | NPA | |
| Li | 0.431 | 0.817 | 0.11 | $Be^{\bullet+}$ | 0.664 | 1.528 | 0.36 | $Zn^{+\cdot}$ | 0.793 | 1.397 | −0.22 |
| Na | 0.629 | 0.841 | −0.05 | $Mg^{\bullet+}$ | 0.942 | 1.510 | −0.20 | $Cd^{\bullet+}$ | 0.955 | 1.300 | −0.44 |
| K | 0.894 | 0.921 | −0.05 | $Ca^{\bullet+}$ | 1.460 | 1.792 | 0.04 | $Hg^{\bullet+}$ | 0.911 | 1.109 | −0.48 |
| Rb | 0.036 | 0.058 | 0.96 | $Sr^{\bullet+}$ | 1.203 | 1.790 | 0.27 | | | | |
| Cs | −0.037 | 0.006 | 1.04 | $Ba^{\bullet+}$ | 1.318 | 1.720 | 0.40 | | | | |

## Discussion

### The nature of the $^2B_2$ states

The calculated charges and spin densities are shown in Table 6. With the exceptions of M = Rb and Cs, for which the $^2B_2$-state simply represents an $s \rightarrow p$ excitation on the metal atom, the NPA-charges confirm the electron-transfer interpretation of the nature of the $^2B_2$ states, although this is not as clear from the Mulliken charges. The Group XII metals also give lower total charges on the metal ions than Group II, supporting the idea that the $^2B_2$ states for these metals have considerable metallacyclopropane character. However, the calculated spin densities demonstrate clearly that electron (and spin) transfer to the ethylene moiety has occurred. Once again, the high negative spin densities found for the Group XII metals suggest different bonding to the Group II complexes. Figure 2 shows the calculated (CCSD/6-311 + G(d,p)) spin density for $^2B_2$ Li:ethylene. The unpaired electron clearly occupies the ethylene $\pi^*$ orbital, polarized toward the lithium ion.

The situation is similar for $^2B_2$ Be:ethylene$^{\bullet+}$, as shown in Fig. 3, except that the beryllium is more heavily involved in the C–Be bonding, making the electron transfer less complete than in the lithium case.

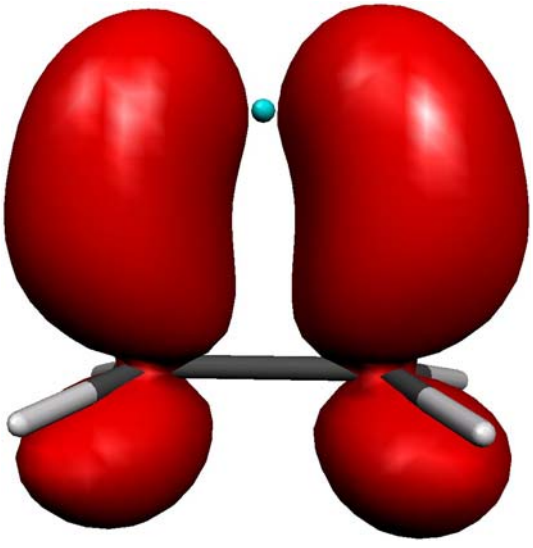

**Fig. 3** Calculated (CCSD/6-311 + G(d,p)) spin density for $^2B_2$ Be:ethylene$^{\bullet+}$. The isodensity level is 0.005 a.u

An analogous plot for $^2B_2$ Zn:ethylene$^{\bullet+}$, is shown in Fig. 4. It is generally similar to that for M = Li but shows more significant contributions from the metal ion.

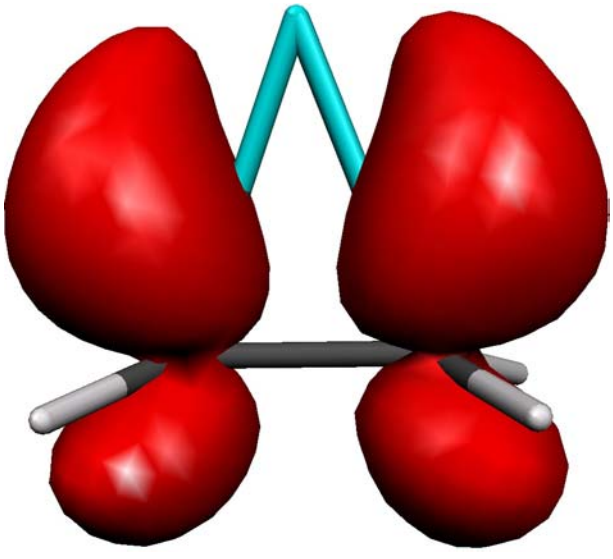

**Fig. 2** Calculated (CCSD/6-311 + G(d,p)) spin density for $^2B_2$ Li:ethylene. The isodensity level is 0.005 a.u

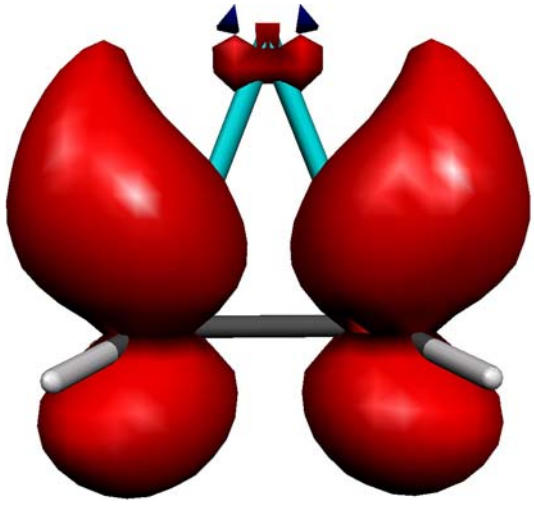

**Fig. 4** Calculated (CCSD/6-311 + G(d,p)) spin density for $^2B_2$ Zn:ethylene$^{\bullet+}$. The isodensity level is 0.005 a.u

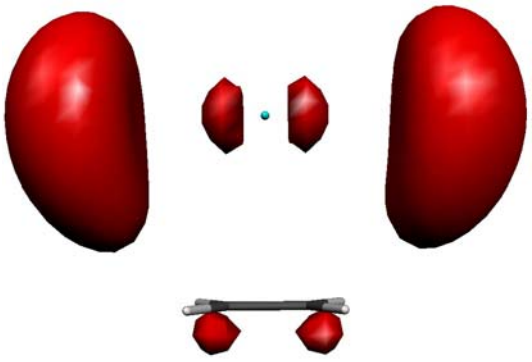

**Fig. 5** Calculated (CCSD/6-311+G(d,p)) spin density for $^2B_2$ Cs:ethylene. The isodensity level is 0.0005 a.u

Finally, Fig. 5 shows an analogous plot for the $^2B_2$ state of Cs:ethylene. As suggested above, this state does not involve electron transfer but is rather a complex of the $^2P$ state of the metal atom.

## Electron-transfer energies

The electron-transfer process from the metal atom or ion to the ethylene moiety can be visualized as a combination of the processes shown schematically in Scheme 2. Conceptually, the electron-transfer process consists of the following individual steps

- Separation of the $^2A_1$ complex to give the separated ethylene and metal components ($-\Delta E_{Comp.}$)
- Ionization of the metal atom or ion ($IP_M$)
- Reduction of the $C_2H_4$ moiety ($-EA_{C_2H_4} = +41.4$ kcal mol$^{-1}$ [40, 41])
- Formation of the ion pair ($E_{Coulomb}$)

The electron-transfer energy, $\Delta E_{ET}$ is thus given by

$$\Delta E_{ET} \simeq -\Delta E_{Comp} + IP(M) - EA_{C_2H_4} + E_{Coulomb} \quad (1)$$

Thus, because $EA_{C_2H_4}$ is constant and by introducing the approximation that $E_{Coulomb}$ is inversely proportional to the C–M distance in the $^2B_2$ complex, we can propose that $\Delta E_{ET} - IP(M) + \Delta E_{Comp.}$ should be proportional to the reciprocal of the C–M distance and that the intersect should correspond to $EA_{C_2H_4}$. Figure 6 shows the corresponding plot for all metals that undergo electron transfer in the $^2B_2$ state.

Although Groups I and XII only contain three valid points, the correlations are at least convincing for Groups I and II. The intersects are clearly not equal, even at the 99% confidence level, so the electron affinity of ethylene is clearly affected by the proximity of a metal ion. However, the intersects are of the correct order. Similarly, a naïve view would expect the slope for Groups II and XII to be twice that for Group I (because the metal ion is doubly charged for groups II and XII). The factor between Groups I and II is found to be 2.4, whereas the slope for Group XII is too poorly defined to be able to make comparisons.

Thus, Fig. 6 supports qualitatively the simple relationship expressed in Eq. 1 and thus the interpretation of the electron-transfer process depicted in Scheme 2. The simple model is, however, not adequate for quantitative predictions unless the slope and the intersect are treated as empirical parameters for each group of the periodic table. Nevertheless, Fig. 6 does support the proposal that the Coulomb ion-paring energy plays a dominant role in determining the reducing ability of metal atoms and ions. This is of course not a proof of the dominance of the Coulomb term. It is, however, difficult to imagine another attractive force with an $r^{-1}$ dependence in these systems. The poor correlation found for Group XII may either be a consequence of only having three points very close to each other, but may also reflect the difference in the basis sets compared with the calculations for the other metals.

## The ground states of Li:$C_2H_4$ and Be:$C_2H_4^{\bullet+}$

Our calculations suggest that the ground states of Li:$C_2H_4$ and Be:$C_2H_4^{\bullet+}$ are both $^2A_1$. These results

**Scheme 2** Schematic energy diagram showing the components of the electron-transfer energy

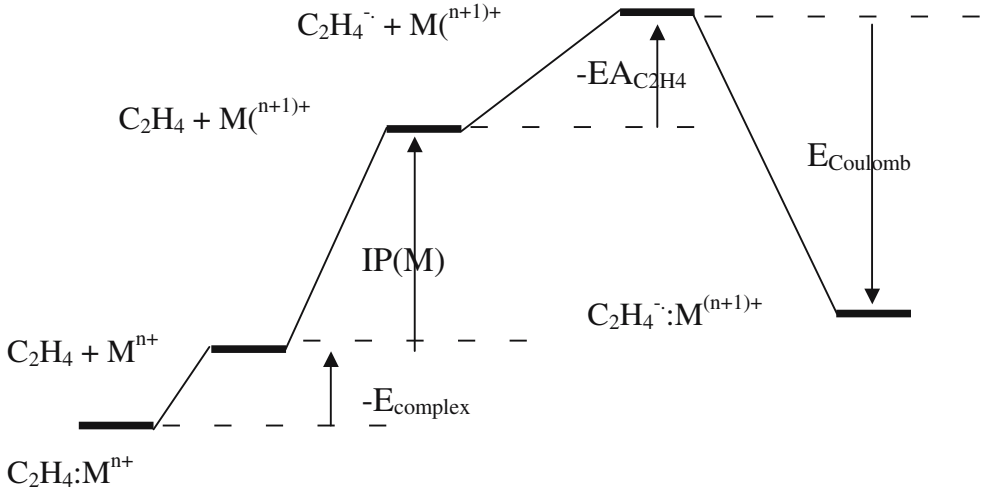

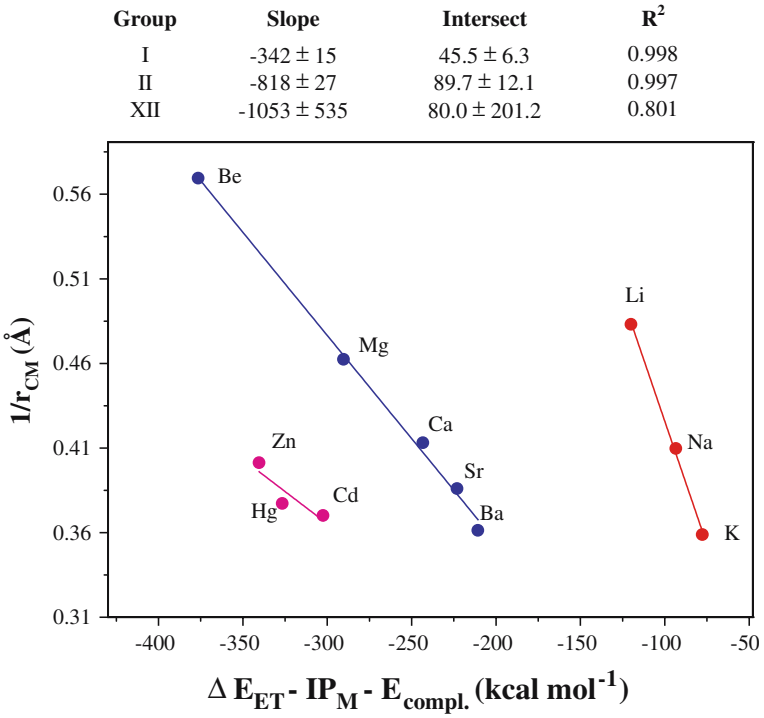


**Fig. 6** Plot of $\Delta E_{ET}$ −IP(M) + $\Delta E_{Comp}$ vs. $1/r_{CM}$ for the metals that give electron transfer in the $^2B_2$ state. CCSD(t)/6-311 + G(d,p)//CCSD/6-311 + G(d,p) calculated energies with an unscaled CCSD/6-311 + G(d,p) ZPE correction were used throughout. The regression equations are listed above

contrast with earlier calculations [10, 12] and experiments in an argon matrix, [13–14] which found $^2B_2$ to be the ground state. Although the energy difference found here is very small (< 3 kcal mol$^{-1}$) for both metals, so that we cannot assign the ground states unequivocally, our calculations are the highest level yet reported for these systems and at least indicate that the ground state in vacuo is not as clearly $^2B_2$ as the earlier work suggests. In our earlier paper [11], we found a significant solvent effect favoring the $^2B_2$ state over the $^2A_1$, but were unable to perform geometry optimizations with solvent simulation. We have therefore now investigated the geometries and relative energies of the two metal complexes in argon solvent using the PCM model for the CCSD/6-311 + G(d,p) geometry optimizations [42]. We originally suggested [11] that the cavity effect would be important in making the $^2A_1$ state more compact because of its very flat energy hypersurface. The results of the PCM optimizations, shown in Table 7, support this hypothesis. The C–Li distance in the $^2A_1$ complex decreases from 4.651 Å in vacuo to 2.837 Å in the argon solvent. This is primarily an effect of the cavity compressing the very flexible C...M distance. The total solvation energy of the $^2A_1$ complex is −2.9 kcal mol$^{-1}$, compared with −5.8 kcal mol$^{-1}$ found for the $^2B_2$ ion pair. Thus, the argon matrix, as expected, favors the ionic structure slightly, making the two configurations essentially energetically degenerate in the argon matrix. Adding the triples correction to the CCSD energy would make the calculated energy difference even smaller. Thus, our calculations suggest that the $^2A_1$ and $^2B_2$ states are very close in energy in vacuo and that solvation in an argon matrix favors the $^2B_2$ ion pair by roughly 2.9 kcal mol$^{-1}$. Our results are thus compatible with the experimental detection of a $^2B_2$ state but not with the results of earlier calculations [10, 12], which suggest that $^2B_2$ is clearly the ground state in vacuo. We suggest, however, that the differences are primarily due to the smaller basis sets used in the earlier calculations.

The geometries of the Be : ethylene$^{\bullet+}$ complexes are less strongly affected by solvation than the very weakly bound $^2A_1$Li:ethylene complex. The C...Be distances become slightly longer in the argon solution. As for Li,

**Table 7** Calculated (CCSD/6-311 + G(d,p)) geometries and energies for Li:$C_2H_4$ and Be:$C_2H_4^{\bullet+}$ within $C_{2v}$ symmetry using a PCM [42] simulation for argon as solvent. The geometrical variables are designated as for Tables 2 and 4

| | $^2A_1$ | $^2B_2$ |
|---|---|---|
| M = Li | | |
| C = C (Å) | 1.343 | 1.436 |
| C...M (Å) | 2.837 | 2.103 |
| ∠CCH (°) | 121.5 | 119.6 |
| ∅M...CCH (°) | 90.5 | 104.1 |
| Total energy (a.u.) | −85.81106 | −85.81048 |
| Solvation energy (kcal mol$^{-1}$) | −2.91 | −5.77 |
| Relative energy (kcal mol$^{-1}$) | 0.00 | 0.36 |
| M = Be$^{\bullet+}$ | | |
| C = C (Å) | 1.361 | 1.459 |
| C...M (Å) | 2.138 | 1.769 |
| ∠CCH (°) | 121.2 | 119.3 |
| ∅M...CCH (°) | 92.0 | 102.3 |
| Total energy (a.u.) | −92.75367 | −92.74736 |
| Solvation energy (kcal mol$^{-1}$) | −22.94 | −27.59 |
| Relative energy (kcal mol$^{-1}$) | 0.00 | 3.97 |

the $^2B_2$ state is stabilized preferentially relative to the $^2A_1$, in this case by roughly 5 kcal mol$^{-1}$. This preferential stabilization would suffice to make the $^2B_2$ ion pair the more stable configuration at the CCSD(T) level.

## Summary and conclusions

Our results suggest that, despite more sophisticated binding possibilities such as contributions from metallacyclopropane structures, the simple redox/electrostatic model given in Scheme 2 and Eq. 1 does a remarkably good job of rationalizing electron-transfer energies between ethylene and the Group I metal atoms or Group II and XII radical cations considered here. The dominant effect of the Coulomb ion-pairing energy means that, for instance, $Be^{\bullet+}$ and $Li^{\bullet}$ are similar in their abilities to reduce ethylene. Our results suggest that diffuse-augmented basis sets favor the $^2A_1$ states relative to the $^2B_2$ ion pairs because BSSE with smaller basis sets favors the ion pairs by stabilizing the $C_2H_4^{\bullet-}$ moiety with excess basis functions from the metal. PCM calculations reveal a small preferential stabilization for the $^2B_2$ ion pairs in argon matrices. Finally, NPA charges and Mulliken spin densities give more reliable descriptions of the electronic structures of these complexes than Mulliken charges, which underestimate the charge separation.

**Acknowledgements** This work was supported by the Deutsche Forschungsgemeinschaft as part of Sonderforschungsbereich 583, Redox-Active Metal Complexes: Control of Reactivity via Molecular Architecture. We thank Dr. Matthias Hennemann for the spin-density plots.

## References

1. Alex A, Clark T (1992) J Am Chem Soc 114:506–510
2. Alex A, Clark T (1992) J Am Chem Soc 114:10897–10902
3. Clark T (1996) Ab initio calculations on electron-transfer catalysis by metal ions. In: Mattay J (ed) Topics in current chemistry, vol 77, electron transfer II. Springer, Berlin Heidelberg New York, pp 1–24
4. Kochi JK (1991) In: Dötz KH, Hoffmann RW (eds) Organic synthesis via organometallics. Vieweg, Braunschweig, pp 95–117
5. Chanon M, Julliard M, Poite JC (1989) Paramagnetic organometallic species in actiovation/selectivity catalysis, NATO ASI Series. Kluwer, Dordrecht
6. Trogler WC (1990) J Organomet Chem Lib 22:306–337
7. Astruc D (1991) Acc Chem Res 24:36–42
8. Chanon M, Rajzmann M, Chanon F (1990) Tetrahedron 46:6193–6299
9. Williams BA, Cool TA (1991) J Chem Phys 94:6358–6366
10. Trenary M, Schaefer III HF, Kollmann PA (1978) J Chem Phys 68:4047–4050
11. Hänsele E, Clark T (1991) Z Phys Chem 171:21–31
12. Alikhani ME, Hannachi Y, Manceron L, Boutelier Y (1995) J Chem Phys 1103:1028–1036
13. Manceron L, Andrews L (1985) J Am Chem Soc 107:563–568
14. Manceron L, Andrews L (1988) J Am Chem Soc 110:3840–3846
15. Rodriguez-Monge L, Larsson S (1996) J Chem Phys 105:7857–7863
16. Bernardi F, Bottoni A, Fossey J, Sorba J (1989) J Mol Struct THEOCHEM 52:301–309
17. White JC, Cave RJ, Davidson ER (1988) J Am Chem Soc 110:6308–6314
18. Balaji V, Jordan KD (1988) J Phys Chem 92:3101–3105
19. Frisch MJ, Trucks GW, Schlegel HB, Scuseria GE, Robb MA, Cheeseman JR, Montgomery JA Jr, Vreven T, Kudin KN, Burant JC, Millam JM, Iyengar SS, Tomasi J, Barone V, Mennucci B, Cossi M, Scalmani G, Rega N, Petersson GA, Nakatsuji H, Hada M, Ehara M, Toyota K, Fukuda R, Hasegawa J, Ishida M, Nakajima T, Honda Y, Kitao O, Nakai H, Klene M, Li X, Knox JE, Hratchian HP, Cross JB, Bakken V, Adamo C, Jaramillo J, Gomperts R, Stratmann RE, Yazyev O, Austin AJ, Cammi R, Pomelli C, Ochterski JW, Ayala PY, Morokuma K, Voth GA, Salvador P, Dannenberg JJ, Zakrzewski VG, Dapprich S, Daniels AD, Strain MC, Farkas O, Malick DK, Rabuck AD, Raghavachari K, Foresman JB, Ortiz JV, Cui Q, Baboul AG, Clifford S, Cioslowski J, Stefanov BB, Liu G, Liashenko A, Piskorz P, Komaromi I, Martin RL, Fox DJ, Keith T, Al-Laham MA, Peng CY, Nanayakkara A, Challacombe M, Gill PMW, Johnson B, Chen W, Wong MW, Gonzalez C, Pople JA (2004) Gaussian 03. Gaussian Inc, Wallingford
20. Cizek J (1969) Adv Chem Phys 14:35–89
21. Purvis GD, Bartlett RJ (1982) J Chem Phys 76:1910–1918
22. Scuseria GE, Janssen CL, Schaefer HF III (1988) J Chem Phys 89:7382–7387
23. Scuseria GE, Schaefer HF III (1989) J Chem Phys 90:3700–3703
24. McLean AD, Chandler GS (1980) J Chem Phys 72:5639–5648
25. Krishnan R, Binkley RS, Seeger R, Pople JA (1980) J Chem Phys 72:650–654
26. Blaudeau J-P, McGrath MP, Curtiss LA, Radom L (1997) J Chem Phys 107:5016–5021
27. Wachters AJH (1970) J Chem Phys 52:1033–1036
28. Hay PJ (1977) J Chem Phys 66:4377–4384
29. Raghavachari K, Trucks GW (1989) J Chem Phys 91:1062–1065
30. Clark T, Chandrasekhar J, Spitznagel GW, Schleyer PvR (1983) J Comp Chem 4:294–301
31. Frisch MJ, Pople JA, Binkley JS (1984) J Chem Phys 80:3265–3269
32. Dunning TH Jr, Hay PJ (1976) In: Schaefer HF III (ed) Modern theoretical chemistry, vol 3. Plenum, New York, pp 1–28
33. Wedig U, Dolg M, Stoll H, Preuss H (1986) In: Veillard A (ed) Quantum chemistry: the challenge of transition metals and coordination chemistry. Reidel, Dordrecht and references therein
34. Pople JA, Head-Gordon M, Raghavachari K (1987) J Chem Phys 87:5968–5675
35. Kaldor U (1987) J Chem Phys 87:4693–4695
36. Raghavachari K, Trucks GW (1989) J Chem Phys 91:2457–2460
37. Iron MA, Oren M, Martin JML (2003) Mol Phys 101:1345–1361
38. Clark T (1988) J Am Chem Soc 110:1672–1678
39. Hiberty PC, Humbel S, Archirel P (1994) J Phys Chem 98:11697–11704
40. Jordan KD, Burrow PD (1978) Chem Phys Lett 36:594–598
41. Jordan KD, Burrow PD (1978) Acc Chem Res 11:341–348
42. Cossi M, Scalmani G, Rega N, Barone V (2002) J Chem Phys 117:43–54
43. Emsley J (1989) The elements. Clarendon Press, Oxford
44. Reed AE, Curtiss LA, Weinhold F (1988) Chem Rev 88:899–926